ISSN 0915-633X

NATIONAL INSTITUTE FOR FUSION SCIENCE

Anomalous Crater Formation in Pulsed-Laser-Illuminated Aluminum Slab and Debris Distribution

T. Yabe, H. Daido,T. Aoki, E. Matsunaga and K. Arisawa

(Received - Apr. 19, 1996)

NIFS-417 May 1996

RESEARCH REPORT
NIFS Series

NAGOYA, JAPAN

Anomalous Crater Formation in Pulsed-Laser-Illuminated Aluminum Slab and Debris Distribution

T. Yabe[a], H. Daido[b] ,T. Aoki[a], E. Matsunaga[a] and K. Arisawa[b]

[a]*Department of Energy Sciences, Tokyo Institute of Technology*
4259 Natatsuta, Midori-ku, Yokohama 226,Japan
[b]*Institute of Laser Engineering, Osaka University*
2-6 Yamada-oka,Suita, Osaka, Japan

Abstract

We have succeeded for the first time to simulate dynamic phase transition from metal to vapor. The crater size created by 650 mJ laser in 8nsec agrees well with the simulation including an elastic-plastic effect and its depth is 100μm which corresponds to anomalously large cutting speed of 10^6 cm/sec for 8ns pulse. However, the simulation demonstrates that evaporation is caused by remnant hot gas during several 100 ns and occurs in the direction of 75 degree in an intermittent and unstable manner leading to a unique explanation on the angular distribution of debris.

Keywords : Laser, Phase Transition, Cutting, Simulation

Recently there has been a growing interest in laser generated debris from a solid target related to x-ray sources for lithography and microscope[1] , femtosecond laser-matter interaction, the prepulse inprint problem in laser fusion, industrial application and so on. However, a numerical scheme to attack such dynamic processes has been beyond the capability of conventional one. In order to simulate these processes, we need a scheme that can simultaneously treat the dynamic evaporation process from metal to liquid and vapor, surface tension, elastic-plastic effect and so on. The major difficulty is to treat a very sharp interface between metal and vapor numerically. The Lagrangean representation is a convenient way to treat a sharp interface but can not be used for the case when the topology changes : the metal surface is melted and flies away as a droplet from the surface. The Eulerian representation with a fixed grid system is another choice to be considered but the numerical diffusion did not permit the use of it at sharp interface. The second problem is to simultaneously treat multi-materials adjacent each other which have different acoustic impedance like liquid and gas.

Recently we have proposed a unique scheme[2] to overcome these difficulties and succeeded for the first time to simulate dynamic phase transition from metal to liquid and gas. The code has been applied to various problems like laser-material processing[3], Shoemaker-Levy 9[4], vapor explosion[5] and so on.

In this letter, we demonstrate that the code can give a unique physical insight into number of interesting features such as crater formation mechanism and angular distribution of debris in an

experiment performed at the Institute of Laser Engineering, Osaka University regarding the x-ray source development[6]. The experiment was performed in a configuration shown in Fig.1 : a YAG laser of 650 mJ in 8nsec is used to obliquely illuminate an aluminum slab target with an angle of 45 degree to the target normal. The same target was used for many shots by rotating and translating it around the axis so that the fresh surface is illuminated in each shot. Debris collectors of glass plates are located 3 cm from the target to measure the angular and size distribution. The diameter of a laser heated plasma is 200 μm observed with an x-ray pinhole camera filtered with a 0.2 μm thick Aluminum. Figure 2 shows an overview of the typical crater obtained in the experiment and simulation. The diameter of the crater is almost the same as that of x-ray picture and the depth is about 100 μm. This crater depth seems to be anomalous because the cutting speed is 100 μm/ 8nsec$\sim 10^6$ cm/sec if this crater should have been created during laser pulse. Since the speeds of sound wave and elastic wave inside aluminum are order of 10^5 cm/sec, the cutting speed is much larger than these speeds. Is this speed physically possible? This question is the starting point of the present work and its answer will be given below.

Figure 3 shows the time development of density contour from hydrodynamic calculation including thermal conduction, viscosity, elastic-plastic effect[7], surface tension[8] , equation of state (EOS) [9] and laser energy deposition. It is interesting to note that the crater is not formed during the laser pulse, but it develops gradually in the time scale of several 100 ns well after the laser pulse ended. The very high

temperature plasma more than a few tens of eV produced by the 8 ns laser pulse and most of them expands from the target. However, some of them still stay near the target for long time after the laser pulse because of recoil force from expanded plasmas and act as heat source to melt aluminum metal in the time scale of several 100 ns. Note that the energy required to make 100 μm crater is only 10 mJ and is only a few percent of laser energy. Therefore, only a small portion of energy remained after bulk expansion is enough to create the crater.

When the plasma temperature becomes less than melting temperature around 290 nsec (the time is measured from the laser peak) , the stress of aluminum whose strength is 0.248 Mbar and yield strength is 2.2976 kbar is recovered and no distortion occurs after that time. This yield stress is quite important to determine the final crater size. Without yield strength, the crater develops further even after 490 ns and the depth becomes more than 300 μm although less difference is seen at the beginning around 90 ns.

The plasma heated crater formation leads to other interesting phenomena. Since the plasma acts not only as heat source but also as pressure source, the dynamic expansion of evaporated material at later time is strongly modified. Since a high pressure region is just in front of the evaporation surface, the vapor is forced to flow bypassing through a narrow channel between the metal surface and this pressure source. Therefore, the vapor preferentially flows toward a circumference with a large angle to the target normal. This effect is the exactly the same as that obtained in the experiment. Figure 4 shows a distribution of

debris from the targets. The histogram is the experimental result and it was drawn from 2000 shots accumulated. The distribution was obtained using an interference microscope by measuring the thickness of aluminum piled-up on the glass plate with an accuracy of 0.01 μm and then getting volume combined with the area measured by a microscope. The estimated error in the distribution is a few tens of percent and is small enough to compare with the simulation result. Clearly there exist two peaks around 0 and 75 degree. As in Fig.3, the plasma expands directed normally to the target at early time t<90 ns and this expansion is a bulk part of the laser-heated plasma. As already stated, this expansion causes recoil force to the hot plasma surrounding aluminum surface. This main part of the expansion creates a peak at 0 degree. The triangles in Fig.4 show the distribution calculated from the time integration of mass flow ru up to t=90 ns. At an early stage t<90 ns, no peak appears around 75 degree. On the other hand, the expansion at later stage t>90nsec is limited to the sideward direction as stated before and creates the peak at 75 degree. Therefore accumulated distribution up to 490 ns shown by circles in Fig.4 increases mainly at 75 degree.

Although the simulation succeeded to replicate the two peaks at 0 and 75 degree, it failed to replicate a narrow distribution at 0 degree, where the simulation result shows a broad distribution. This broad distribution already started in the distribution accumulated up to 90 ns and perhaps is mainly due to an early time behavior of expansion during laser heating. We are not sure whether this difference is caused by some unknown mechanism to collimate the hot plasma expansion

or angular dependence of reflectivity at the collector plate. In the experimental result, we have assumed 100 % adhesion to the plate.

Simulation also predicts further interesting behavior. The expansion at t<40nsec is quite uniform because its temperature is quite high ~a few tens of eV. The experiment supports this result and the debris around 0 degree is very fine and indistinguishable with an optical microscope. On the other hand, the simulation result at t=290 nsec shows some filamentary streams flowing from the surface. The experiment also supports this result and the debris at 75 degree consists of 1 to 20 μm sized particles. Since the simulation is two-dimensional axisymmetric, we cannot estimate the particle size but we can suggest the origin of the filaments.

The evaporated gas at later time must flow through a very narrow channel to the circumference and therefore this narrow channel creates thermal insulation layer between metal surface and heat source. Then heat flow is instantaneouly suppressed reducing evaporation. If the evaporation is suppressed, the narrow channel disappears and the heat source directly contact the metal surface. Thus the heat flow from heat source to metal surface is recovered causing again evaporation and the formation of narrow channel of thermal insulation layer. Repeating this process, the intermittent evaporation occurs and the filamentary streams appear as shown in Fig.3. Although the detailed time evolution is not seen from Fig.3, the animation picture shows that, during flight to vacuum, condensation occurs from low density clouds to well defined filaments seen in Fig.3 at 290 ns.

The phenomena analyzed here implies the very important effect in short-pulse, high-intensity laser-matter interaction. Even if the laser pulse is short and is not sufficiently long to create the crater, the remaining high temperature plasma can play a role to create a large crater if the laser intensity is sufficiently high ($\sim 10^{12}$ W/cm^2 in the present case). Most importantly, we now have a very useful tool to analyze the dynamic phase transition and related instabilities.

This work was carried out under the collaborating research program at the National Institute for Fusion Science of Japan. This work was supported by Light-Quantum Project at Japan Atomic Energy Research Institute, Matsuo Foundation, and Ministry of Education.The experimental aspect of this work was partly supported by the Institute of Laser Technology. The authors are indebted to Prof.S.I.Anisimov for his userful discussion and to Profs. Y.Kato, Y.Izawa and S.Nakayama for their support to this experiment.

References

[1] M.L.Ginter and T.J.Mcllrath, Appl.Opt. 27, 885 (1988) ; I.C.E.Turcu *et al.*, Proc. Soc. Photo-Opt. Instrum. Eng. 1503, 391 (1991) ; G.D.Kubiak *et al.*, OSA Proc. Soft X-Ray Projection Lithography Vol.18 ed. by A.M.Hawryluk and R.H.Stulen (Optical Society of America, Wahington. D.C., 1993) p.127.

[2] H.Takewaki, T.Yabe, J.Comput.Phys. 70, 355(1987); T.Yabe and T.Aoki, Comput. Phys. Commun. 66, 219 (1991); T.Yabe and P.Y.Wang, J.Phys.Soc.Japan 60, 2105 (1991).

[3] T.Yabe, Rev.Laser Engrg. 20, 691 (1992).

[4] T.Yabe *et al.*, Geophy.Res.Lett. 22, 2429 (1995).

[5] T.Yabe and F.Xiao, Nucl. Eng. Des. 155, 45 (1995).

[6] G.M.Zeng, H.Daido *et al.*, J.Appl.Phys. 69, 7460(1991) ; J.Appl.Phys. 72, 3355 (1992) ; J.Appl.Phys. 75, 1923(1994).

[7] M.L.Wilkins, "*Calculation of Elastic-Plastic Flow*" in Methods in Computational Physics Vol.3, p.211 (Academic Press, 1964).

[8] J.U.Brackbill, D.B.Kothe and C.Zemach, J.Comput. Phys. 100, 335 (1992)

[9] The EOS is modified from that used in ref.3 with Clausius-Clapeyron's law considering latent heat in the region of two phases.

Figure Captions

Fig.1 : Experimental configuration. An aluminum slab target is placed in a vacuum chamber of 5×10^{-5} Torr and the debris collector is located 3cm from the target.

Fig.2 : Typical shape of the crater obtained (left) from the experiment and (right) from the simulation, where the left half of each figure is aluminum.

Fig.3 : Top, middle and bottom figures show density contours at 40 ns, 90 ns, and 290 ns from the laser peak. In the figures, laser light is incident from the right and logarithmic density is shown : purple, green, yellow, red show the density of 2.7, 10^{-2}, 10^{-3}, background density ($<10^{-4}$) g/cm^3, respectively. The vertical length of the figure is 800 μm.

Fig.4 : Debris distribution. 0 degree corresponds to the target normal. The histogram shows the experimental result, while circles and triangles show the accumulated mass from the simulation at 490 ns and 90 ns, respectively.

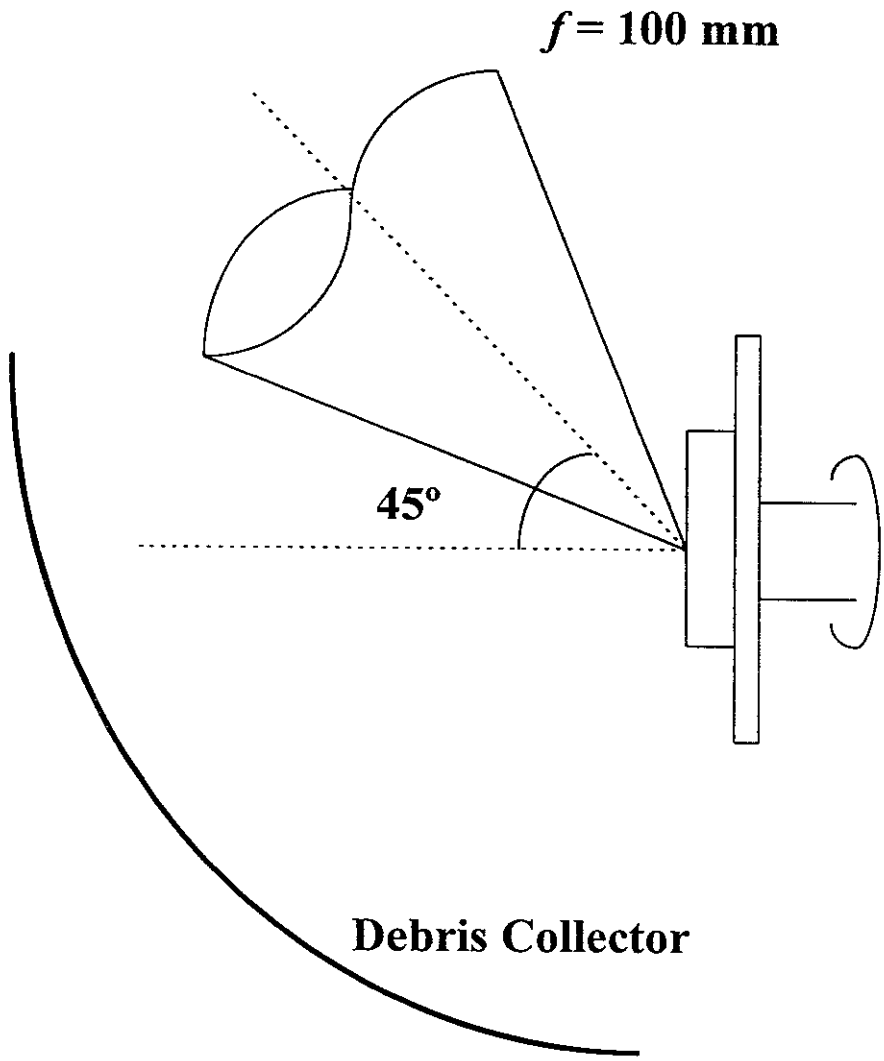

Fig.1

Fig.2

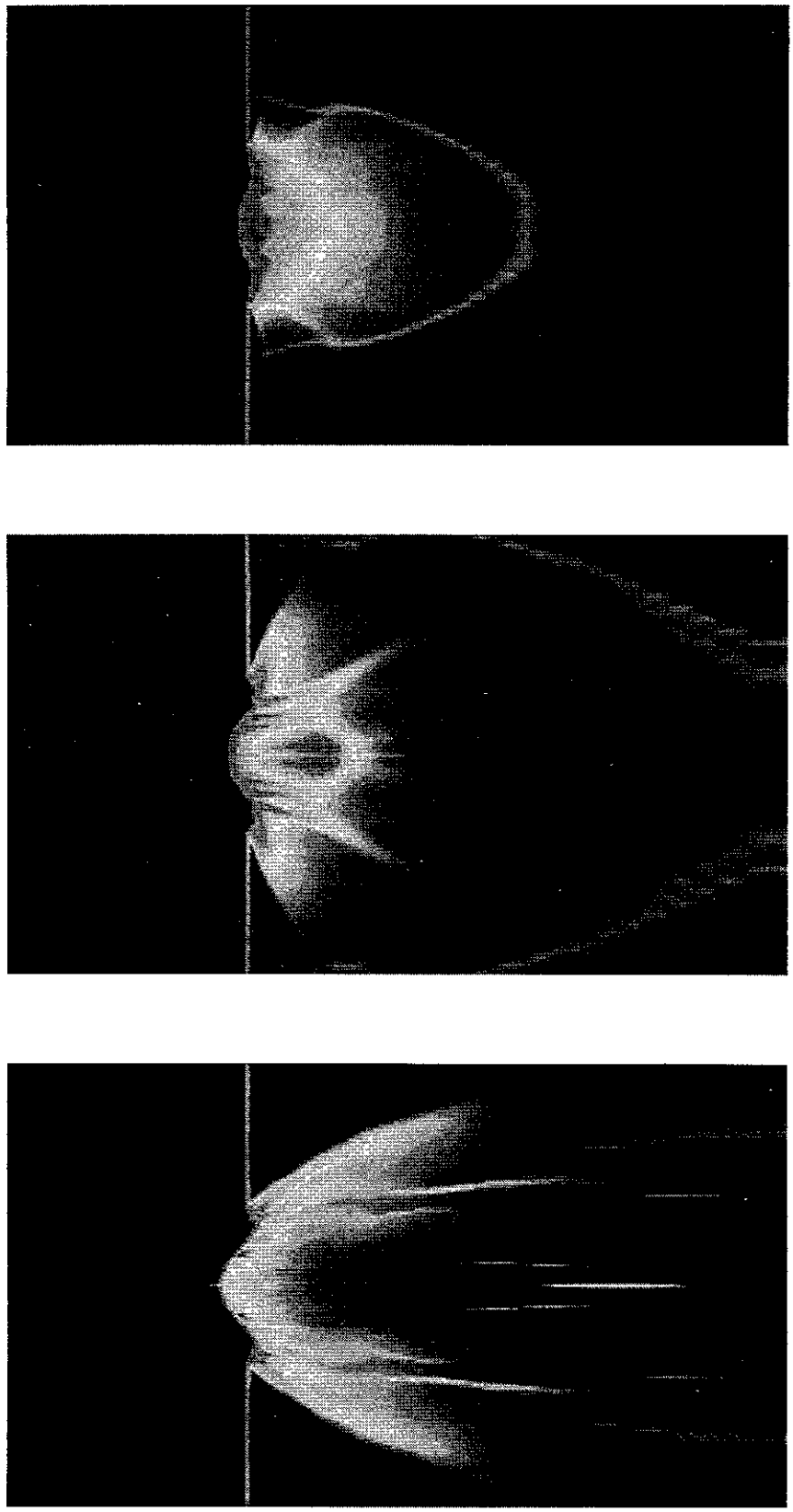

Fig.3

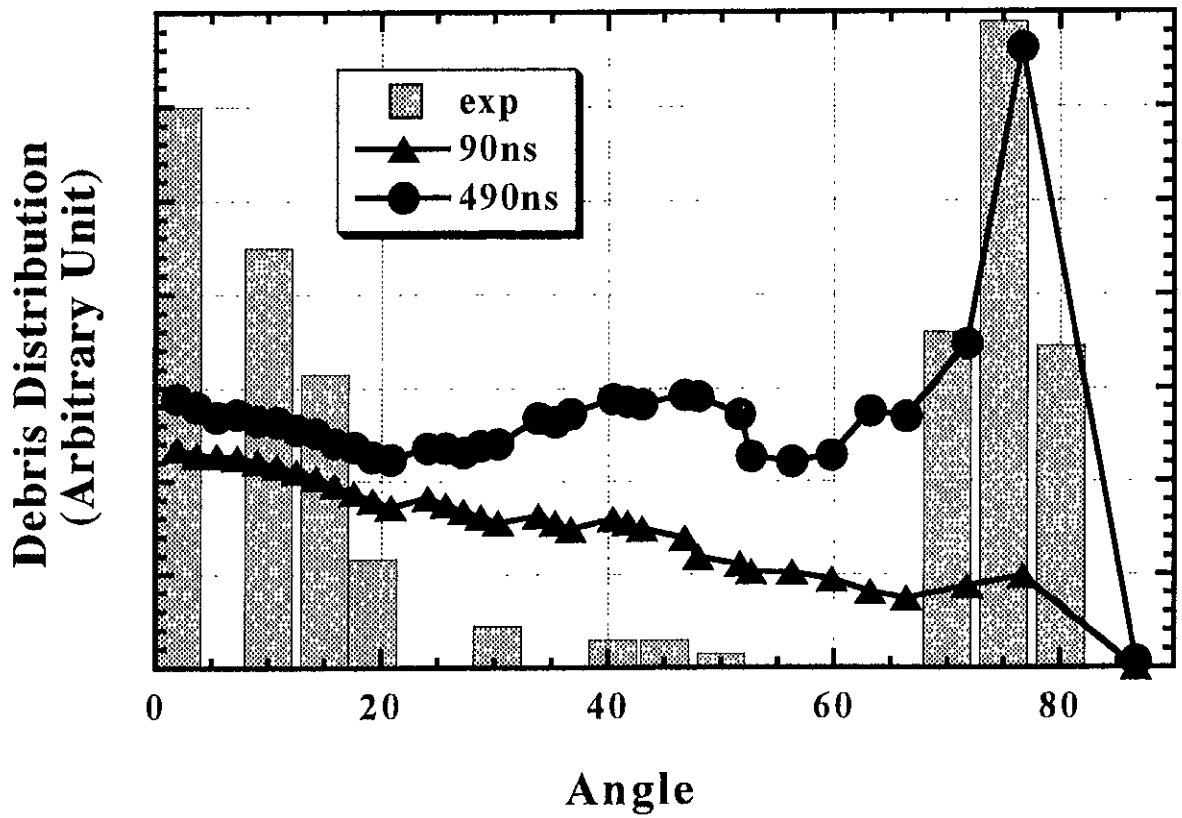
exp
90ns
490ns
Debris Distribution
(Arbitrary Unit)
0
20
40
60
80
Angle

Fig.4

Recent Issues of NIFS Series

NIFS-370 M. Sasao, A. Taniike, I. Nomura, M. Wada, H. Yamaoka and M. Sato,
Development of Diagnostic Beams for Alpha Particle Measurement on ITER; Aug. 1995

NIFS-371 S. Yamaguchi, J. Yamamoto and O. Motojima;
A New Cable -in conduit Conductor Magnet with Insulated Strands; Sep. 1995

NIFS-372 H. Miura,
Enstrophy Generation in a Shock-Dominated Turbulence; Sep. 1995

NIFS-373 M. Natsir, A. Sagara, K. Tsuzuki, B. Tsuchiya, Y. Hasegawa, O. Motojima,
Control of Discharge Conditions to Reduce Hydrogen Content in Low Z Films Produced with DC Glow; Sep. 1995

NIFS-374 K. Tsuzuki, M. Natsir, N. Inoue, A. Sagara, N. Noda, O. Motojima, T. Mochizuki, I. Fujita, T. Hino and T. Yamashina,
Behavior of Hydrogen Atoms in Boron Films during H_2 and He Glow Discharge and Thermal Desorption; Sep. 1995

NIFS-375 U. Stroth, M. Murakami, R.A. Dory, H. Yamada, S. Okamura, F. Sano and T. Obiki,
Energy Confinement Scaling from the International Stellarator Database; Sep. 1995

NIFS-376 S. Bazdenkov, T. Sato, K. Watanabe and The Complexity Simulation Group,
Multi-Scale Semi-Ideal Magnetohydrodynamics of a Tokamak Plasma; Sep. 1995

NIFS-377 J. Uramoto,
Extraction of Negative Pionlike Particles from a H2 or D2 Gas Discharge Plasma in Magnetic Field; Sep. 1995

NIFS-378 K. Akaishi,
Theoretical Consideration for the Outgassing Characteristics of an Unbaked Vacuum System; Oct. 1995

NIFS-379 H. Shimazu, S. Machida and M. Tanaka,
Macro-Particle Simulation of Collisionless Parallel Shocks; Oct. 1995

NIFS-380 N. Kondo and Y. Kondoh,
Eigenfunction Spectrum Analysis for Self-organization in Dissipative Solitons; Oct. 1995

NIFS-381 Y. Kondoh, M. Yoshizawa, A. Nakano and T. Yabe,
Self-organization of Two-dimensional Incompressible Viscous Flow

in a Friction-free Box; Oct. 1995

NIFS-382 Y.N. Nejoh and H. Sanuki,
The Effects of the Beam and Ion Temperatures on Ion-Acoustic Waves in an Electron Beam-Plasma System; Oct. 1995

NIFS-383 K. Ichiguchi, O. Motojima, K. Yamazaki, N. Nakajima and M. Okamoto
Flexibility of LHD Configuration with Multi-Layer Helical Coils;
Nov. 1995

NIFS-384 D. Biskamp, E. Schwarz and J.F. Drake,
Two-dimensional Electron Magnetohydrodynamic Turbulence; Nov. 1995

NIFS-385 H. Kitabata, T. Hayashi, T. Sato and Complexity Simulation Group,
Impulsive Nature in Collisional Driven Reconnection; Nov. 1995

NIFS-386 Y. Katoh, T. Muroga, A. Kohyama, R.E. Stoller, C. Namba and O. Motojima,
Rate Theory Modeling of Defect Evolution under Cascade Damage Conditions:The Influence of Vacancy-type Cascade Remnants and Application to the Defect Production Chracterization by Microstructural Analysis; Nov. 1995

NIFS-387 K. Araki, S. Yanase and J. Mizushima,
Symmetry Breaking by Differential Rotation and Saddle-node Bifurcation of the Thermal Convection in a Spherical Shell; Dec. 1995

NIFS-388 V.D. Pustovitov,
Control of Pfirsch-Schlüter Current by External Poloidal Magnetic Field in Conventional Stellarators: Dec. 1995

NIFS-389 K. Akaishi,
On the Outgassing Rate Versus Time Characteristics in the Pump-down of an Unbaked Vacuum System; Dec. 1995

NIFS-390 K.N. Sato, S. Murakami, N. Nakajima, K. Itoh,
Possibility of Simulation Experiments for Fast Particle Physics in Large Helical Device (LHD); Dec. 1995

NIFS-391 W.X.Wang, M. Okamoto, N. Nakajima, S. Murakami and N. Ohyabu,
A Monte Carlo Simulation Model for the Steady-State Plasma in the Scrape-off Layer; Dec. 1995

NIFS-392 Shao-ping Zhu, R. Horiuchi, T. Sato and The Complexity Simulation Group,
Self-organization Process of a Magnetohydrodynamic Plasma in the Presence of Thermal Conduction; Dec. 1995

NIFS-393 M. Ozaki, T. Sato, R. Horiuchi and the Complexity Simulation Group
Electromagnetic Instability and Anomalous Resistivity in a Magnetic

Neutral Sheet; Dec. 1995

NIFS-394 K. Itoh, S.-I Itoh, M. Yagi and A. Fukuyama,
Subcritical Excitation of Plasma Turbulence; Jan. 1996

NIFS-395 H. Sugama and M. Okamoto, W. Horton and M. Wakatani,
Transport Processes and Entropy Production in Toroidal Plasmas with Gyrokinetic Eletromagnetic Turbulence; Jan. 1996

NIFS-396 T. Kato, T. Fujiwara and Y. Hanaoka,
X-ray Spectral Analysis of Yohkoh BCS Data on Sep. 6 1992 Flares - Blue Shift Component and Ion Abundances -; Feb. 1996

NIFS-397 H. Kuramoto, N. Hiraki, S. Moriyama, K. Toi, K. Sato, K. Narihara, A. Ejiri, T. Seki and JIPP T-IIU Group,
Measurement of the Poloidal Magnetic Field Profile with High Time Resolution Zeeman Polarimeter in the JIPP T-IIU Tokamak; Feb. 1996

NIFS-398 J.F. Wang, T. Amano, Y. Ogawa, N. Inoue,
Simulation of Burning Plasma Dynamics in ITER; Feb. 1996

NIFS-399 K. Itoh, S-I. Itoh, A. Fukuyama and M. Yagi,
Theory of Self-Sustained Turbulence in Confined Plasmas; Feb. 1996

NIFS-400 J. Uramoto,
A Detection Method of Negative Pionlike Particles from a H2 Gas Descharge Plasma; Feb. 1996

NIFS-401 K.Ida, J.Xu, K.N.Sato, H.Sakakita and JIPP TII-U group,
Fast Charge Exchange Spectroscopy Using a Fabry-Perot Spectrometer in the JIPP TII-U Tokamak; Feb. 1996

NIFS-402 T. Amano,
Passive Shut-Down of ITER Plasma by Be Evaporation; Feb. 1996

NIFS-403 K. Orito,
A New Variable Transformation Technique for the Nonlinear Drift Vortex; Feb. 1996

NIFS-404 T. Oike, K. Kitachi, S. Ohdachi, K. Toi, S. Sakakibara, S. Morita, T. Morisaki, H. Suzuki, S. Okamura, K. Matsuoka and CHS group;
Measurement of Magnetic Field Fluctuations near Plasma Edge with Movable Magnetic Probe Array in the CHS Heliotron/Torsatron; Mar. 1996

NIFS-405 S.K. Guharay, K. Tsumori, M. Hamabe, Y. Takeiri, O. Kaneko, T. Kuroda,
Simple Emittance Measurement of H- Beams from a Large Plasma Source; Mar. 1996

NIFS-406 M. Tanaka and D. Biskamp,
Symmetry-Breaking due to Parallel Electron Motion and Resultant Scaling in Collisionless Magnetic Reconnection; Mar. 1996

NIFS-407 K. Kitachi, T. Oike, S. Ohdachi, K. Toi, R. Akiyama, A. Ejiri, Y. Hamada, H.Kuramoto, K. Narihara, T. Seki and JIPP T-IIU Group,
Measurement of Magnetic Field Fluctuations within Last Closed Flux Surface with Movable Magnetic Probe Array in the JIPP T-IIU Tokamak; Mar. 1996

NIFS-408 K. Hirose, S. Saito and Yoshi.H. Ichikawa
Structure of Period-2 Step-1 Accelerator Island in Area Preserving Maps; Mar. 1996

NIFS-409 G.Y.Yu, M. Okamoto, H. Sanuki, T. Amano,
Effect of Plasma Inertia on Vertical Displacement Instability in Tokamaks; Mar. 1996

NIFS-410 T. Yamagishi,
Solution of Initial Value Problem of Gyro-Kinetic Equation; Mar. 1996

NIFS-411 K. Ida and N. Nakajima,
Comparison of Parallel Viscosity with Neoclassical Theory; Apr. 1996

NIFS-412 T. Ohkawa and H. Ohkawa,
Cuspher, A Combined Confinement System; Apr. 1996

NIFS-413 Y. Nomura, Y.H. Ichikawa and A.T. Filippov,
Stochasticity in the Josephson Map; Apr. 1996

NIFS-414 J. Uramoto,
Production Mechanism of Negative Pionlike Particles in H_2 Gas Discharge Plasma; Apr. 1996

NIFS-415 A. Fujisawa, H. Iguchi, S. Lee, T.P. Crowley, Y. Hamada, S. Hidekuma, M. Kojima,
Active Trajectory Control for a Heavy Ion Beam Probe on the Compact Helical System; May 1996

NIFS-416 M. Iwase, K. Ohkubo, S. Kubo and H. Idei
Band Rejection Filter for Measurement of Electron Cyclotron Emission during Electron Cyclotron Heating; May 1996

NIFS-417 T. Yabe, H. Daido,T. Aoki, E. Matsunaga and K. Arisawa
Anomalous Crater Formation in Pulsed-Laser-Illuminated Aluminum Slab and Debris Distribution; May 1996